CIB-W18/44-15-4

INTERNATIONAL COUNCIL FOR RESEARCH AND INNOVATION IN BUILDING AND CONSTRUCTION

WORKING COMMISSION W18 - TIMBER STRUCTURES

DESIGN OF BOTTOM RAILS IN PARTIALLY ANCHORED SHEAR WALLS USING FRACTURE MECHANICS

E Serrano

A Olsson

Linnæus University, Växjö

J Vessby

Linnæus University and Tyréns AB, Växjö

U A Girhammar

Luleå University of Technology

B Källsner

Linnæus University, Växjö, and SP Stockholm

SWEDEN

MEETING FORTY FOUR

ALGHERO

ITALY

AUGUST 2011

Design of Bottom Rails in Partially Anchored Shear Walls Using Fracture Mechanics

Erik Serrano[1], Johan Vessby[2], Anders Olsson[1], Ulf Arne Girhammar[3], Bo Källsner[4]

[1]Linnæus University, Växjö, Sweden.
[2]Linnæus University, and Tyréns AB, Växjö, Sweden
[3]Luleå University of Technology, Sweden.
[4] Linnæus University, Växjö, and SP Technical Research Institute of Sweden, Stockholm, Sweden.

1. Introduction

A recent development in the design of medium-rise timber structures relates to the use of plastic design approaches that include three-dimensional effects e.g. Källsner and Girhammar (2006) and Källsner et.al. (2010). One of the greatest benefits with such an approach is that lateral walls connected to the stabilizing shear walls may be used as anchorage to counteract the considerable uplifting forces that may occur at times. On the one hand this design philosophy predicts an enhanced performance of the timber house. On the other hand it may introduce uplifting forces in the bottom rail, which is assumed to be anchored to the substrate. Thus the risk of splitting failure in the bottom rail must be assessed, since if such splitting of the rail occurs in a brittle manner, the plastic design philosophy may be put in question. The aim of the current study is to use the concept of fracture mechanics to establish and verify an analytical expression for the load bearing capacity of a bottom rail anchored to the substrate and exposed to an uplifting force through the sheathing. Such an expression makes it possible to predict the force at which splitting will occur. Bearing in mind that the failure modes are dominated by fracture perpendicular to the fiber direction, fracture mechanics is an appealing approach to use. Fracture mechanics has been successfully applied to other design situations in timber engineering, the best known example perhaps being the formulae of Eurocode 5 for the design of notched beams (Gustafsson 1988).

1.1 Geometry and loading conditions

A shear wall is connected to the substrate through the bottom rail or/and through hold down devices connecting the studs to the substrate. If the bottom rail is used for force transmission of horizontal forces to the substrate, the force is transmitted through dowel action in the anchor bolts and through friction between the rail and the substrate. The anchor bolts are, however, also at times necessary for holding down the rail, i.e. preventing it from lifting. An anchor bolt is placed in a predrilled hole in the wood, through a washer typically placed in the centre of the rail. This implies that an eccentricity is introduced between the uplifting forces from the sheet connected to the bottom rail and the hold down forces in the anchor bolt. If too large forces are introduced this eccentricity may cause a splitting failure in the rail. Two examples of such splitting failure are illustrated in Figure 1(a) for a vertical crack and (b) for a horizontal crack.

The example of the failure modes are shown to the left in the figure and a drawing that shows the geometrical parameters used for analyzing the structural performance of the rail is shown to the right. The failure modes illustrated in Figure 1(a) have been investigated experimentally (Girhammar and Källsner 2009) and an empirical design formula has been suggested

(Girhammar et al. 2010). The formula takes different washer sizes into account, and the failure mode has been studied for sheathing on one or both sides of the rail. However, the phenomenon has not been studied theoretically.

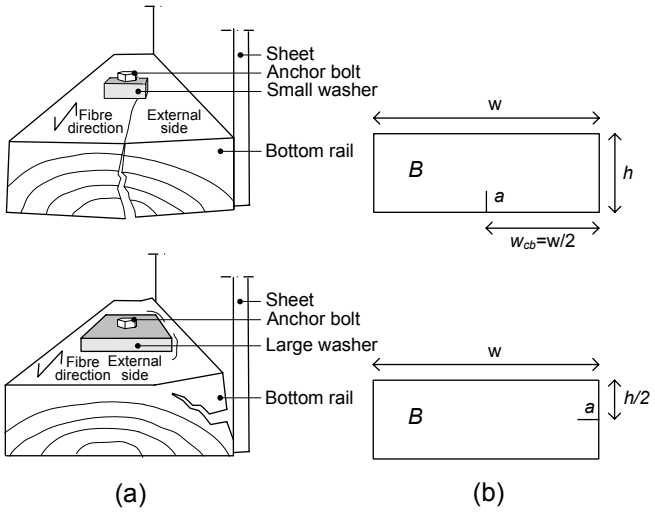

Figure 1. (a) Bottom rail at failure due to splitting. The rail is anchored to the substrate by means of an anchor bolt and a washer. (b) Parameters used in the current study for analyzing the rail.

The exact location of the crack may vary but two major types of failure, see Figure 1, were identified in Girhammar and Källsner (2009). In the current study, it is assumed that the crack initiates either from the bottom tensile edge, at half the width, w of the rail, or from half height of the rail, see Figure 1. The height of the rail is referred to as h, and the out of plane length of the rail, i.e. the "width" of the crack, will be referred to as B. Since the rail length B = 0.9 m was used in the experimental investigation by Girhammar and Källsner (2009), the same length will be used in the current study such that the results may be easily compared.

1.2 Material properties

In order to simplify the analyses of the rail all analyses are performed in two dimensions. It is likely, however, that using a two dimensional model, the predicted load-carrying capacity will be overestimated, since such a model does not take into account the variation in stress distribution in the longitudinal direction of the rail. Stress concentrations prior to fracture probably occur close to the anchor bolt. A three dimensional analysis could be used to evaluate the significance of this, and to suggest some factor that would compensate for it in a two dimensional model, but such an analysis is not presented in this paper. The rail is loaded perpendicular to its length direction, and thus the moduli perpendicular to this, E_R and E_T should be used in analyses performed in the radial-tangential plane (RT-plane). In design codes in general no distinction is made between the R- and T-directions and analyses based on analytical expressions suitable for hand-calculations should therefore preferably make use of only one in-plane modulus of elasticity (MOE). In addition, the shear stiffness in the RT-plane will influence the deformation pattern in the RT-plane. Index r in G_r represents *rolling shear* and the appropriate value to assign for G_r depends on the actual orientation of the annual rings. It is thus not a notation referring specifically to radial direction of the wood material. This rolling shear modulus is typically an order of magnitude lower than the RT-plane MOEs, and can therefore give rise to considerable deformation. In the present study the values of 600 and 500 MPa were chosen for E_R and E_T, respectively. For the cases where the Poisson effect is included, its value was set to ν_{RT} = 0.5. The strength of the timber in tension,

$f_{t,90}$ is set to 2.5 MPa and the critical energy release rate, $G_{IC,}$, is assigned a value representative for pure mode I failure perpendicular to grain, in softwoods. This value was assumed to be constant, G_{IC} = 300 J/m^2, for any crack path in the RT-plane, which is an approximation. The values of the material parameters used herein are given in Table 1.

Table 1. Material data used in the performed analysis.

Material property	Value
E_R	600 MPa
E_T	500 MPa
G_r	50 MPa
ν_{RT}	0.5
$f_{t,90}$	2.5 MPa
G_{IC}	300 J/m^2

The material directions of the wood are assumed to be constant within the timber in the simple hand calculation approach. It is therefore not self-evident what value to use for the elastic parameters when comparing with the results from a 2D FE-model, where the cylindrical nature of the material is taken into account. In an orthotropic material, the effective modulus of elasticity and shear modulus, related to a fixed coordinate system, is shown in Figure 2. As can be seen, the effective values vary considerably with the angle of the material direction to the fixed global directions. In the present work, if nothing else is stated, the set of parameters corresponding to an annual ring orientation of zero degree angle (cf. Figure 2) is used for the hand calculation models. Thus, MOE was set to 500 MPa and rolling shear modulus to 50 MPa.

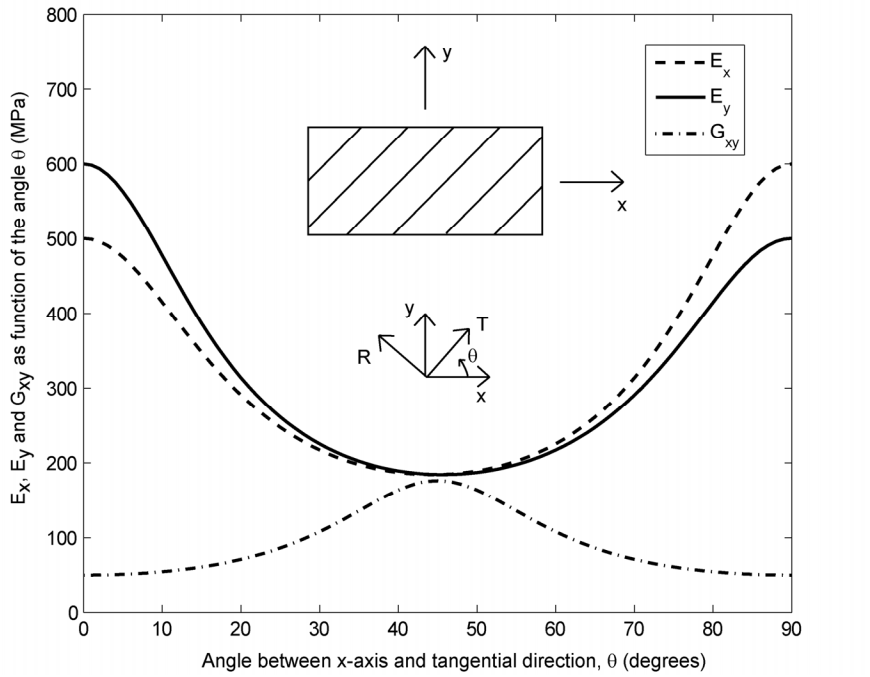

Figure 2. Influence of annual ring orientation on the effective moduli of elasticity and shear modulus referring to the global x-y-coordinate system.

2. Analysis methods

In this section linear elastic fracture mechanics (LEFM) theory leading to a suggested formula for calculating the load bearing capacity of a rail subjected to uplift forces and splitting is presented. In addition, a finite element model for assessing the compliance of the rail in more detail and a non-linear fracture mechanics (FCM) model for comparison are presented.

2.1 Basic LEFM theory – Energy release rate analysis

There are several approaches for analyzing a crack propagating in a material using LEFM. A crack is assumed to propagate when the energy release rate of the body equals the critical energy release rate of the material, G_C. By calculating the energy release rate for increasing crack length, the critical load (failure load) as a function of crack length can be obtained. Here, the so-called compliance method is used. The basis for this method is that, at crack propagation, the stiffness of the system is reduced, or equivalently, the compliance is increased. Details concerning such an approach can be found in e.g. Petersson (2002). For the case of a single point load, P^0, no body forces, and assuming quasi-static conditions, the change of potential energy $(-\Delta\Pi)$ of the system can be calculated

$$-\frac{\partial \Pi}{\partial a} = \frac{1}{2} P^0 \frac{\partial u(P^0,a)}{\partial a} \tag{1}$$

where P^0 is a (constant) reference load acting on the system and a is the current crack length. The change of potential energy is in this case the driving "force" for crack propagation. At crack propagation we conclude that $-d\Pi/da = B \cdot G_C$, where B is the length of the studied rail and G_C is the critical energy release rate of the material.

If the notation P_c is used for the critical load and u_c for the corresponding displacement at the loading point (single point load case) the expression takes the form

$$\frac{P_c}{2}\frac{\partial u_c}{\partial a} = B \cdot G_C \tag{2}$$

With $C = u/P$ being equal to the compliance of the linear elastic structure, we obtain (assuming P being constant during crack propagation)

$$\frac{P_c^2}{2}\frac{\partial C}{\partial a} = B \cdot G_C \tag{3}$$

The value of G_C is strongly dependent on which mode of fracture is involved during crack propagation, and this mode of fracture will in general vary during loading, see Figure 2. For simplicity, here only mode I is taken into account so that $G_C = G_{IC}$. This simplification is practical and in general a safe approach, since $G_{IC} < G_{IIC}$.

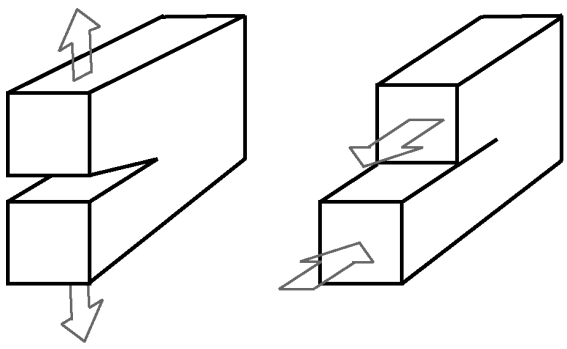

(a) (b)

Figure 3. Mode I (a) and mode II (b) loading.

As mentioned above, a further approximation made for simplicity is that the value of G_{IC} was set as independent of the crack direction in the RT-plane. More of the theory behind the energy release rate criterion may be found in e.g. Haller and Gustafsson (2002), Serrano and Gustafsson (2006) working specifically with wood or any standard text book on linear elastic fracture mechanics for a more general background.

2.2 Energy release rate – simplified hand calculations

Simple hand calculation formulae have been developed for two different assumptions of the position and direction of crack development: a vertical and a horizontal crack respectively.

2.2.1 Vertical crack

For commonly used rail- and washer dimensions the most frequently occurring failure mode is that a vertical crack develops. If the geometry of the studied bottom rail is simplified, the structure can be considered as a cantilever beam with the length w_{cb} and the height *(h-a), h* being the original height of the rail and *a* being the current crack length, see Figure 4.

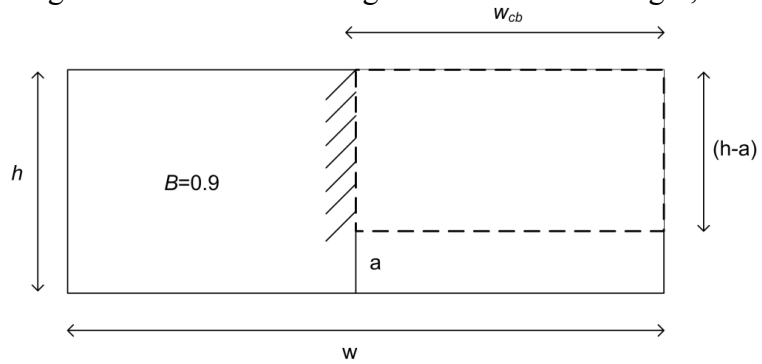

Figure 4. One end of the rail is considered a cantilever beam with the length w_{cb} and the height (h-a).

Once this simplification has been made the compliance of the cantilever beam can be expressed on basis of the bending and shear deformations of such a beam when subjected to a point load at the free end, i.e.

$$C(a) = \frac{4 \cdot w_{cb}^3}{E \cdot B \cdot (h-a)^3} + \frac{\beta \cdot w_{cb}}{G \cdot B \cdot (h-a)} \tag{4}$$

where E is a modulus of elasticity, G is the shear modulus and β is the shear correction factor, equal to 1.2 for a rectangular cross-section. The derivative of the compliance with respect to the crack length is obtained as

$$\frac{\partial C}{\partial a} = \frac{12 \cdot w_{cb}^3}{E \cdot B \cdot (h-a)^4} + \frac{\beta \cdot w_{cb}}{G \cdot B \, (h-a)^2} \tag{5}$$

The displacement, due to the load P, may be expressed as $u=P \cdot C$, and thus (3) may be reformulated to obtain an expression for the critical load. With $G_C = G_{IC}$, $E = E_{90}$ (stiffness in a direction perpendicular to grain, not necessarily coinciding with E_r or E_t) and $G = G_r$ we arrive at

$$P_c = \sqrt{\frac{2 \cdot B \cdot G_{IC}}{\frac{\partial C}{\partial a}}} = (h-a) \cdot B \cdot \sqrt{\frac{2 \cdot G_{IC}}{w_{cb}\left(\frac{12 \cdot w_{cb}^2}{E_{90} \cdot (h-a)^2} + \frac{\beta}{G_r}\right)}} \tag{6}$$

where P_c is the critical load. This equation thus represents the critical load as a function of the crack length, a. Although some approximations were introduced in the derivation of (6), the simple format is appealing. This closed-form solution based on a sound theoretical approach

can be used to investigate the qualitative influence of various parameters. If necessary, (6) could also be calibrated to test results or more advanced analyses based on finite element results, by introducing additional parameters.

2.2.2 Horizontal crack

The second most common failure mode in the studied load case is that a crack develops horizontally from the position of the nails, commonly at half height of the rail. Such a crack would typically initially develop horizontally but would successively change direction so that it reaches the top side of the washer at a 45 degree angle, cf. Figure 1.

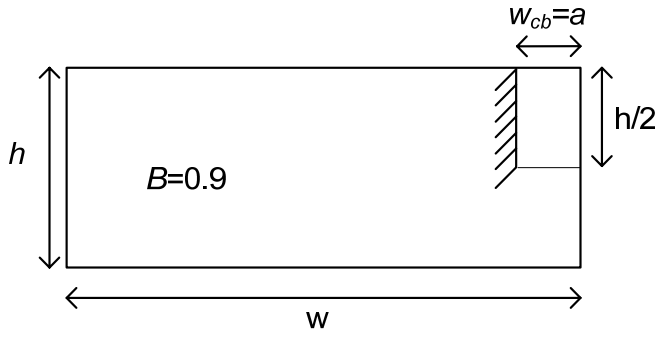

Figure 5. Simplified, one end of the rail may be seen as a cantilever beam with the length, w_{cb}, being equal to the length of the crack, a, and the height h/2.

In Figure 5 a simplified model for hand calculation for that case is suggested assuming a cantilever beam with the height $h/2$ and the length w_{cb} being equal to the length of the crack, a. Such approximation would be relevant for crack lengths less than about 15 mm since the direction of the crack would deviate to much from the suggested horizontal direction. Under these assumptions the compliance may be expressed as

$$C(a) = \frac{4 \cdot a^3}{E \cdot B \cdot \left(\frac{h}{2}\right)^3} + \frac{\beta a}{G_r \cdot B \cdot \left(\frac{h}{2}\right)} \tag{7}$$

using the same notations as was previously suggested for the vertical crack. The derivative of the compliance is obtained as

$$\partial C / \partial a = \frac{96 a^2}{E \cdot B \cdot h^3} + \frac{2\beta}{G_r \cdot B \cdot h} \tag{8}$$

Note that in the derivative of the compliance the shear contribution is constant, i.e. independent of the length of the crack while the contribution from the bending term depends in a quadratic manner on the length of the crack. Making use again of the general expression (3) we now obtain for the horizontal crack

$$P_c = B \cdot h \sqrt{\frac{G_{IC} \cdot G_r \cdot E \cdot h}{48 \cdot G_r \cdot a^2 + \beta \cdot h^2 \cdot E}} \tag{9}$$

For small crack lengths the bending term may be disregarded. Under such assumptions the critical load may be expressed as

$$P_c \approx B \cdot \sqrt{\frac{G_{IC} \cdot G_r \cdot h}{\beta}} \tag{10}$$

2.3 Energy release rate using the finite element method

The aim of the numerical analysis performed using the finite element method is to determine the compliance of the structure in order to calculate the critical load, see (3). This calculation is performed at different stages of the crack propagation. At each stage, the compliance is calculated by determining the displacement, $u_{0,i}$ under a constant load, and this is then repeated for different crack lengths a. The crack propagation length, Δa_i, is set to the side length of a finite element, so that for each propagation of the crack one node is released. For a stage in which node i has been released the corresponding physical crack length is set to

$$a \approx \frac{a_{i+1}+a_i}{2} \tag{11}$$

where a_i is the distance from the edge of the rail to node i and a_{i+1} is the distance from the bottom of the rail to node i+1. Thus the tip of the crack is assumed to be located at the mid-point of the edge of the newly released finite element.

A rail with h = 45 mm and w = 120 mm was loaded with the load P vertically in one degree of freedom at half the height of the right end of the rail. The boundary conditions were set so that the left bottom corner of the rail was pinned and the rest of the left bottom was prescribed to have zero vertical displacement. The boundary condition at the top of the rail was set so that displacement in vertical direction was restrained at the degree of freedom with the eccentricity e from the centre of the rail in order to give a simple condition corresponding to the effect of the washer. The length of the eccentricity of the top boundary condition was set to e_{bc} = 10 mm, a value that could easily be changed. Load, boundary conditions and notations used for width, w, height, h, eccentricity of the top boundary condition, e_{bc}, the distance from the vertical crack to the edge of the washer, e_0, the distance from the edge of the washer to the edge of the rail, e_{edge}, the length of the rail, B, and crack length, a, are all indicated in Figure 6 (a) and (b) respectively.

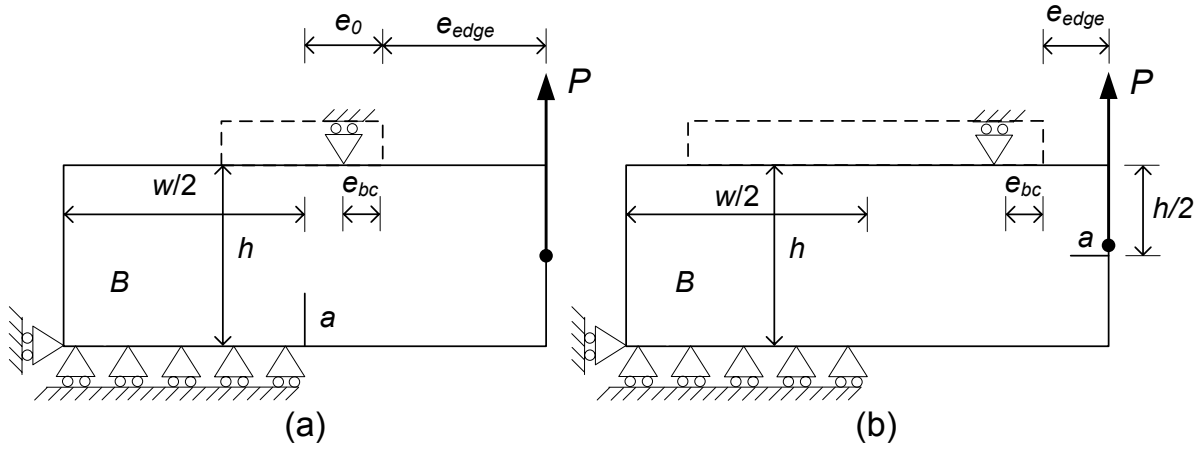

Figure 6. Geometry and applied load case for the studied rail with (a) a vertical crack and (b) a horizontal crack, each with the length a. The position of the washer (substituted by a boundary condition in the analyses) is indicated with dashed lines.

In the hand calculation models the length of the cantilever beam, w_{cb}, will be e_0+e_{edge} for the case with a vertical crack and a for the case of a horizontal crack. In the FEM model using LEFM by contrast, the distance from the edge of the rail to the location of the boundary condition at the top of the rail is e_{edge} +e_{bc} for both cases.

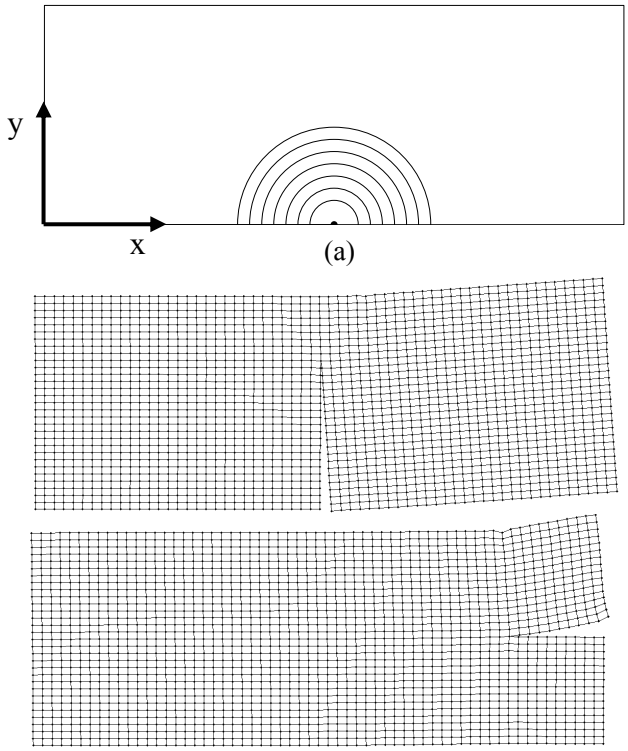

Figure 7. (a) The position of the pith was set to (x,y)= (60,0) mm. (b) The mesh used in the analyses with cracks that have propagated. Deformations are magnified 10 times.

The material was modeled using the orthotropic parameters introduced in Table 1. A cylindrical coordinate system was used to define the material orientation, the origin of this coordinate system being placed at the position (x,y)=(60,0), see Figure 7(a). Rectangular four node linear elements were used in the finite element model. The two-dimensional analyses were performed using the assumption of plane strain state with the length of the rail being 0.90 m. Examples of the meshes used for the analyses are shown in Figure 7(b) showing also the deformed rail, at a load of 1000 N with deformations being magnified 10 times. A total of 60 × 30 elements were used. For the shown states, the crack has propagated to about three quarters of the height of the rail and about 20 mm for the vertical and horizontal cracks, respectively.

2.4 Nonlinear fracture mechanics – fictitious crack model

A nonlinear fictitious crack model (FCM) was implemented as a complement to the hand calculations and the LEFM FE-model. The previously described crack propagation paths were used also in the nonlinear model. The material parameters of the wood material and the origin of the cylindrical coordinate system were set to the same as previously indicated. The characteristics of the crack were obtained assuming linear softening behavior from the strength perpendicular to the fibers, $f_{t,90}$, to the crack opening were no stresses are transmitted, w_c, cf. Figure 8. If the fracture energy and the strength perpendicular to the fibers according to Table 1 is used, the critical tip opening displacement, w_c, may be calculated to 0.24 mm. The same FCM was used for the two different cracks modeled.

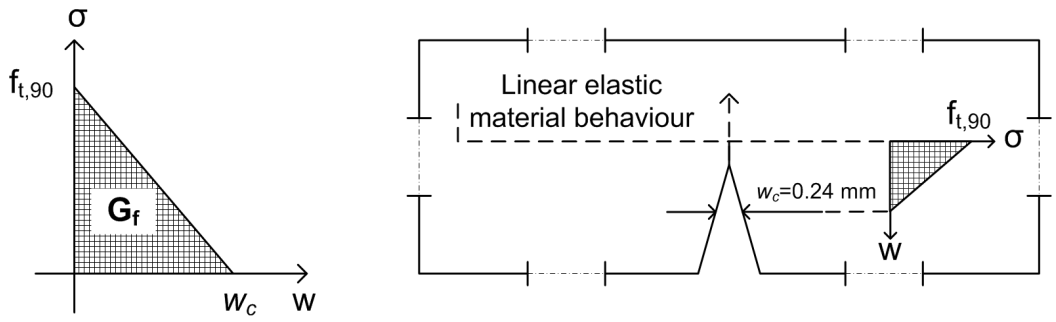

(a) (b)

Figure 8. (a) A linear softening behavior was assumed in the FCM, defining the critical opening displacement, w_c, where no stress can be transmitted. (b) Above the crack, i.e. above the position where the stress level is equal to $f_{t,90}$, the material behaves linearly elastically.

3. Results

In Figure 9 the critical load, P_c, obtained using the closed form expression (6) and the LEFM FE-model, respectively, is plotted as function of the crack length a in case of a vertical crack. The maximum load capacity calculated using the FCM is also indicated in Figure 9 but not as a function of the crack length, as this is not defined in the FCM analysis in a way comparable with the other calculations. On basis of the stress distribution it can be concluded, however, that the crack length is about 6 mm when the maximum load is reached according to the FCM analysis. In Figure 10 the complete course of loading for the FCM analysis is shown. The load is plotted versus the crack mouth opening displacement, CMOD, successively increasing for increasing displacements in the loading point and showing the strongly nonlinear behavior with softening after peak load. Assuming a 6 mm crack length the results from the closed form expression, the LEFM FE-model and the FCM FE-model are 12.4 kN, 12.3 kN and 13.9 kN, respectively. Considering the rough simplifications made there is thus a very good agreement between the different methods of analysis. It may also be noted that the agreement is acceptable between LEFM and the analytical model, i.e. the closed form expression, at least if crack lengths are smaller than 20 mm.

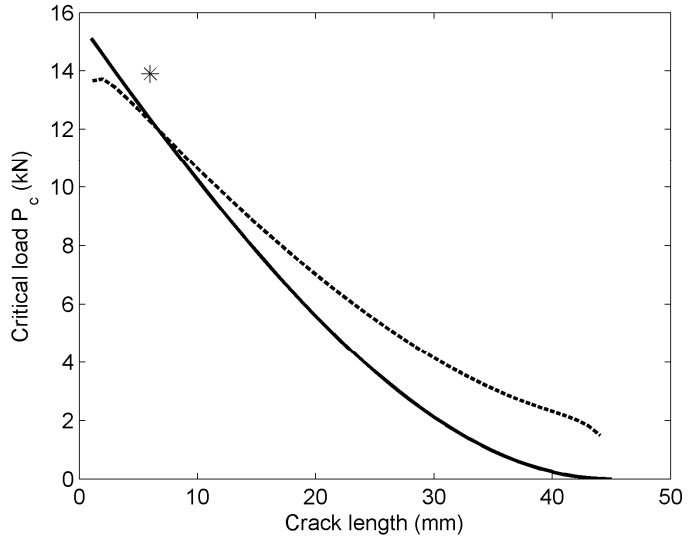

Figure 9. Critical load, P_c, as a function of crack length according to the closed form expression (solid line) and the LEFM FE simulation (dashed), both for the vertical crack. The asterisk indicates the critical load according to the FCM analysis, which appears at a state corresponding to a crack length of about 6 mm.

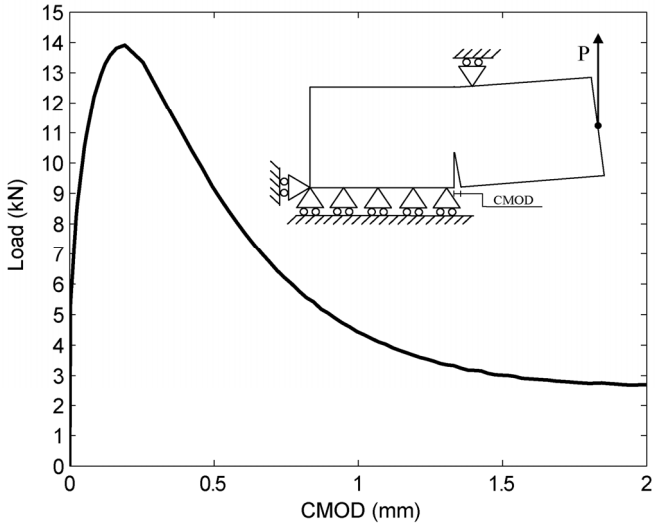

Figure 10. Load in the rail as a function of crack mouth opening displacement, CMOD for the vertical crack. The relation is obtained using the FCM.

In Figure 11 the critical load is shown for increasing crack lengths for the case of a horizontal crack. Similarly to the results from the vertical crack the results from the closed form expression, with and without consideration of bending, and the LEFM model, in this case for the horizontal crack are shown. As discussed earlier, see also Figure 1, the crack referred to as the horizontal crack is only horizontal for a limited crack length, around 15 mm, and thereafter deviates from the horizontal direction. This implies that the models should not be compared for lengths of the crack exceeding this value. In Figure 12 the complete course of loading for the FCM analysis is shown. The peak value, also shown in Figure 11, relates to the crack length 13 mm and the critical load P_c = 21.1 kN.

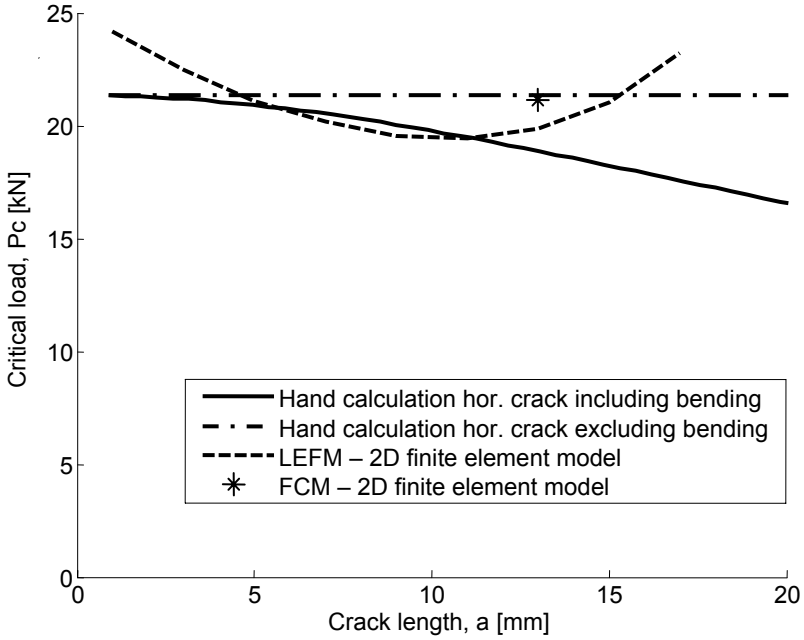

Figure 11. Critical load, P_c,as a function of crack length according to the closed form expression (solid line) and the LEFM FE simulation (dashed), both for the horizontal crack. The asterisk indicates the critical load according to the FCM analysis, which appears at a state corresponding to a crack length of about 13 mm.

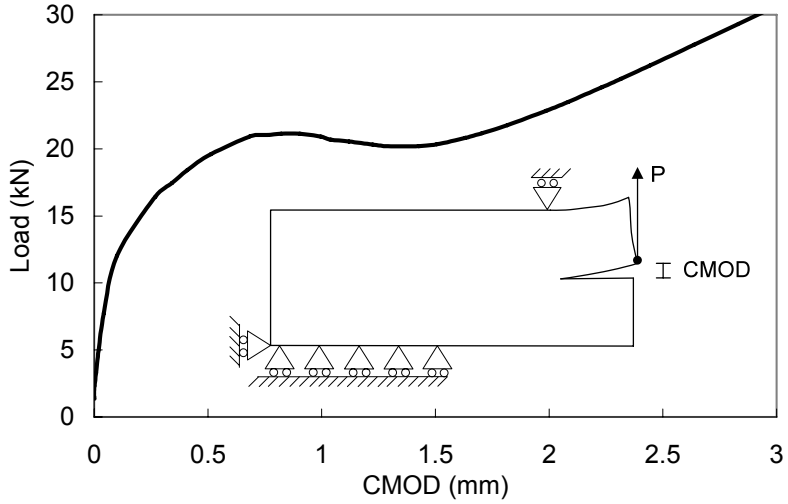

Figure 12. Load in the rail as a function of crack mouth opening displacement, CMOD for the horizontal crack. The relation is obtained using the FCM.

4. Discussion and comparison with experiments

The three different methods employed for analyzing the load capacity in the bottom rail for two different cracks give similar results, at least if the crack length, *a*, is not too large in relation to the in-plane dimensions of the rail. This is of course promising with respect to the usefulness of the simple, closed form expression developed above. However, the calculated results and the models employed should be compared and assessed by means of experimental results. Such experiments were performed (Girhammar et al. 2010) for different sizes and location of washers and for single and double sided sheathing on the rail. The critical failure load in the single-sided test with the smallest size of the washer, that being 40 mm wide, was found to be 12.1 kN for the vertical crack. This agrees rather well with the calculated values, see Figure 9.

Since the purpose was to establish a simple expression that could be used for hand calculation, some simplifications were made in the analytical model leading to the closed form expressions. One such simplification is the choice of the length of the cantilever in the model. This length could be considered a fitting parameter, taking into account a number of different factors such as the size and shape of the washer, the friction between the substrate and the rail, pretension of the anchor bolt and how the load *P* is introduced to the rail.

Another parameter to consider is the length of an assumed initial crack, *a*. Using *a=0,* the simplest possible way of expressing the critical load for the vertical crack would be

$$P_c = h \cdot B \cdot \sqrt{\frac{2 \cdot G_{IC}}{w_{cb}\left(\frac{12 \cdot w_{cb}^2}{E_{90} \cdot h^2} + \frac{\beta}{G_r}\right)}} \tag{12}$$

For the horizontal crack, *a=0* would correspond to not considering the bending contribution, see eq. 10. Using *a=0* would, however, lead to an overestimation of the critical load. Instead the choice of crack length to be used should preferably be estimated according to theoretical considerations related to the so-called initial crack method (Serrano and Gustafsson 2006). The proper crack length to use is (for pure mode I) according to this theory:

$$a_c = \frac{E_{90} \cdot G_{IC}}{\pi \cdot f_t^2} \tag{13}$$

In the present case, this would correspond to a crack length of 7.6 mm. The results from the FCM-analysis of the vertical crack indicated that the crack length at maximum load is about 6 mm, somewhat smaller than according to the suggested theory. Using (6) with an initial crack according to (13) would result in

$$P_c = \left(h - \frac{E_{90} \cdot G_{IC}}{\pi \cdot f_t^2}\right) \cdot B \cdot \sqrt{\frac{2 \cdot G_{IC}}{\left(\frac{12 \cdot w_{cb}^3}{E_{90} \cdot \left(h - \frac{E_{90} \cdot G_{IC}}{\pi \cdot f_t^2}\right)^2} + \frac{w_{cb} \beta}{G_r}\right)}} \tag{14}$$

which is a closed-form expression for the critical load with a theoretically sound basis. Note also that the approximate expression for the horizontal crack when disregarding the contribution from bending, see (10), is independent of the crack length.

In Girhammar et al. (2010) an *empirical* expression for the critical load as a function of the distance from the side of the washer to the edge of the rail is presented. Those results are compared with the expressions developed in the present work in Figure 13. The results from the analytical models in Figure 13 were obtained with E=400 MPa and G=70 MPa, which in turn corresponds to an average annual ring orientation of 10-15°, cf. Figure 2.

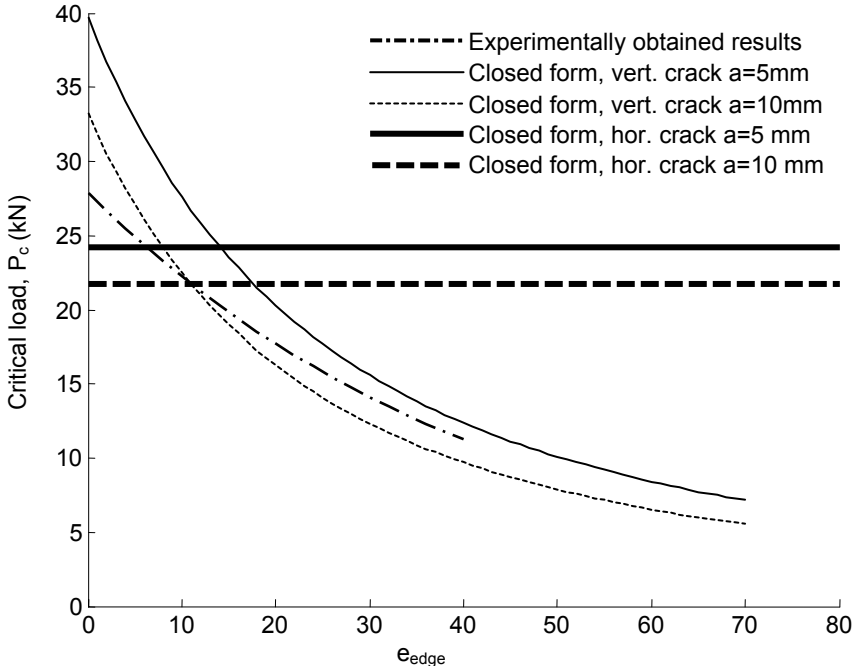

Figure 13. Comparison of results according to an empirical expression based on experiments and according to analytical models (eqs. 6 and 9). The curves show critical load versus length from washer edge to rail edge, e_{edge}. Washer size is here 40 mm. Horizontal curves correspond to a horizontal crack (eq.9.)

The agreement between the curves based on the analytical model and the curve based on experimental results is good. The larger the edge distance, the better the agreement with the assumption of a vertical crack, while shorter edge distances give a better agreement with model predictions based on the assumptions of a horizontal crack. Note that the results shown in Figure 13 were obtained without calibrating to the actual material parameters, nor to the

annual ring orientations in the tests. In addition to such calibration, the length of the cantilever to be used in the analytical model could be used as a calibrating parameter.

5. Conclusions

The aim of the current study was to establish and verify a simple analytical expression that could be used to obtain the design load for vertically loaded rails fixed to the ground using washers. This was done by comparing analytical expressions to finite element models using LEFM and the FCM, respectively. The analytical expressions were also verified by a previously experimentally obtained expression. Good agreement could be found for the analytical expression in all cases indicating that they have potential for inclusion in the code. Some conclusions can be drawn from the study:

Although rather crude simplifications were used to establish the analytical expressions for the critical load, P_c , good agreement was found between the crack models and the two different fracture mechanic models, one linear and the other nonlinear, based on finite element modeling.

The length of the cantilever beam can be used as a fitting parameter, taking into account a broad range of parameters such as the geometry of the washer, the friction between rail and the substrate the pretension of the anchor bolt and the way that the load P is introduced.
The current study covers only one load case and should therefore not be generalized without further verification.

6. References

Girhammar, U. A., Källsner, B. (2009). "Design aspects on anchoring the bottom rail in partially anchored wood-framed shear walls" *Proc. CIB-W18 meeting*, Duebendorf, Switzerland, paper 42-15-1.

Girhammar, U. A., Källsner, B., Daerga, P-A. (2010). "Recommendations for design of anchoring devices for bottom rails in partially anchored timber frame shear walls" *Proc. World conference on timber engineering,* Trentino, Italy.

Gustafsson, P. J. (1988). "A study of strength of notched beams" *Proc. CIB-W18 meeting*, Vancouver, Canada, paper 21-10-1.

Haller, P., Gustafsson, P.J. (2002). "An overview of fracture mechanics concepts." *Fracture mechanics models for strength analysis of timber beams with a hole or a notch – a report of RILEM TC-133*, P. J. Gustafsson, ed. TVSM-7134, Lund, Sweden.

Källsner, B., Girhammar, U. A. (2006) "A plastic design method for incompletely anchored wood-framed wall diaphragm" *Proc. World conference on timber engineering,* Portland, Oregon, USA.

Källsner, B., Girhammar, U. A., Vessby, J. (2010) "Some design aspects on anchoring of timber frame shear walls by transverse walls" *Proc World conference on timber engineering*, Riva del Garda, Italy.

Petersson, H. (2002). "Energy release rate analysis." Fracture mechanics models for strength analysis of timber beams with a hole or a notch – a report of RILEM TC-133, P. J. Gustafsson, ed., TVSM-7134, Lund, Sweden.

Serrano, E., Gustafsson, P. J. (2006) "Fracture mechanics in timber engineering – Strength analyses of components and joints", *Materials and Structures*, 40(1), 87-96.